Progress In Electromagnetics Research, Vol. 114, 301–315, 2011

AN EFFICIENT HYBRID TECHNIQUE FOR ANALYSIS OF THE ELECTROMAGNETIC FIELD DISTRIBUTION INSIDE A CLOSED ENVIRONMENT

V. P. Bui, X. C. Wei, E. P. Li, and W. J. Zhao

A*STAR Institute of High Performance Computing
1 Fusionopolis Way, #16–16 Connexis, 138632, Singapore

Abstract—This paper presents an efficient hybrid simulation technique for analysis of the electromagnetic field interactions between multi-transmitters and receivers located within a closed environment. The Method of Moments/circuit method is first used for modeling of the transceivers and their nearby surrounding to obtain the equivalent sources/receivers. Then, an approach that combines the asymptotic method and the ray tracing technique is deployed to calculate the long-distance coupling between a pair of transmitter and receiver. The acceleration algorithms for ray tracing have been developed to deal with more complex scenarios. The seamless combination between the circuit, numerical, and asymptotic approaches is the key to get accurate simulation results. Several numerical examples and experimental results are presented to demonstrate the efficiency of the proposed technique.

1. INTRODUCTION

The ability to accurately predict the electromagnetic field distribution within a closed environment plays a significant role in the industrial applications such as aircraft cabin, below-desk compartments in ship, automotive interior, reverberation chamber, etc. Indeed, this permits the calculation of the received signal strengths for radio coverage planning and the interference prediction for the analysis of electromagnetic compatibility (EMC) [1–3]. The simulation technology is attractive because it is far less costly compared to the long, labor-intensive measurement campaigns, and easily adapts for different

Received 21 January 2011, Accepted 28 February 2011, Scheduled 2 March 2011
Corresponding author: Viet Phuong Bui (buivp@ihpc.a-star.edu.sg).

environment setups. However, the difficulties for modeling faced in such a closed environment are due to the multi-frequency band and multi-scale of the whole closed environment. The devices used for different purposes cover a wide frequency spectrum from kHz up to GHz, and the overall dimension of a closed environment is extremely huge in comparison with the smaller devices used inside. It is a big challenge for available simulators based on single modeling techniques to fully solve these difficult problems. Indeed, the full-wave numerical simulation techniques such as Method of Moments (MoM), Finite Element Method (FEM) or Finite-Difference-Time-Domain (FDTD), although accurate, become computational expensive as the computer storage and computing time will grow rapidly at high frequencies. On the other hand, asymptotic approaches such as Physical Optics (PO), Geometric Optics (GO) or Uniform Theory of Diffraction (UTD), although fast, are not accurate for modeling the small objects and the structural details [4–7].

Therefore, we propose an efficient hybrid technique, which will benefit from both numerical and asymptotic approaches and overcome their drawbacks. Our simulation technique makes a full use of the structural features of the closed environment. It decomposes the original complex problem into several kinds of simple sub-problems [8–11]. Thereafter, these sub-problems are solved by using different optimized approaches respectively, and then recombined by the equivalent sources defined on their interfaces [12]. The efficiency of the hybrid technique is demonstrated through several numerical and experimental examples.

2. HYBRID SIMULATION TECHNIQUE

A pair of transmitter and receiver is usually designed as highly resonant structures with the same resonant frequency in order to efficiently transfer the electromagnetic wave. Under their resonant modes, their working parameters, such as the resonant frequency and the input impedance, are primarily affected by their nearby regions. Based on this, suitable circuit/numerical approaches are used to accurately simulate the transceivers and their nearby regions. The results obtained are then taken as the equivalent source/receiver and substituted into the asymptotic approach that efficiently calculates the long-distance coupling between the transmitter and receiver.

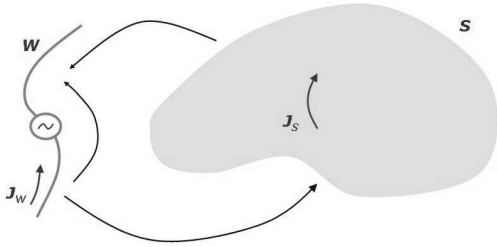

Figure 1. Antenna and its adjoining object.

2.1. Modeling of the Transceivers

The transmitting/receiving antenna and its adjoining objects in free-space as shown in Figure 1 are modeled based on the integral equation

$$\vec{E}^{inc} - L_S(\vec{r},\vec{r}')\vec{J}_S(\vec{r}') - L_W(\vec{r},\vec{r}')\vec{J}_W(\vec{r}')\Big|_t = \begin{cases} Z_s\vec{J}_S(\vec{r})/2 \\ Z_s\vec{J}_W(\vec{r})/4\pi a \end{cases}, \vec{r}\in S,W; \tag{1a}$$

and the operator L_{S_α} is given by

$$L_{S_\alpha}\vec{J}_{S_\alpha}(\vec{r}) = jk\eta_0\int_{S_\alpha} dS(\vec{r}')(\vec{J}_{S_\alpha}(\vec{r}')+1/k^2\nabla\nabla'\cdot\vec{J}_{S_\alpha}(\vec{r}'))G(\vec{r},\vec{r}'),\ S_\alpha = S,W, \tag{1b}$$

where subscript t denotes the component tangential to S and W; $\vec{J}_W$ and $\vec{J}_S$ are the electric current densities on W and S, respectively; $\vec{E}^{inc}$ represents the incident electric field; $G(\vec{r},\vec{r}') = e^{-jk|\vec{r}-\vec{r}'|}/4\pi|\vec{r}-\vec{r}'|$ is the free-space Green's function; $|\vec{r}-\vec{r}'|$ is the distance between the field point $\vec{r}$ and the source point $\vec{r}'$; $k = 2\pi/\lambda$, where λ is the wavelength; η_0 is the free space impedance; a is the radius of the wires; Z_s is the surface impedance which considers the effect of coating materials on objects and the skin-effect of metal at high frequency.

Solving (1) by using MoM, the whole structure is discretized into small segments/triangles. $\vec{J}_W$ and $\vec{J}_S$ are then expanded by using the RWG basic functions defined on each pair of segments/triangles [13–15]. In this way, by using Galerkin testing method, we can obtain the following linear equations

$$[Z]\begin{Bmatrix} I_W \\ I_S \end{Bmatrix} = \{e\}, \tag{2}$$

where I_W and I_S denote the unknown current expansion coefficients of $\vec{J}_W$ and $\vec{J}_S$, respectively. $\{e\}$ is the antenna feed.

To efficiently fill $[Z]$, and $[e]$ of (2), the interactions between each pair of triangles/segments are first calculated, and then these results are added to the corresponding elements in all matrices of (2). This is called *element-based* matrix filling method. It actually reduces the matrices filling time. To do so, we need to redefine half-RWG basic functions for each triangle and segment:

$$\vec{f}_{i.m}(\vec{r}) = \begin{cases} \frac{1}{2A_i}(\vec{r} - \vec{r}_{i,m}), & m = 1,2,3 \quad \text{and} \quad \vec{r} \in triangle\, T_i \\ \frac{1}{l_i}(\vec{r} - \vec{r}_{i,m}), & m = 1,2 \quad \text{and} \quad \vec{r} \in segment\, l_i \end{cases}, \quad (3)$$

where A_i is the area of triangle T_i, l_i is the length of the segment l_i, and $\vec{r}_{i,m}$ is the three/two nodes of the triangle/segment.

Equation (2) can be solved by using the computer, then $\vec{J}_W$ and $\vec{J}_S$ can be obtained. After that, the radiation/receiving field from the transmitting/receiving antenna can be calculated as

$$\vec{E} = -L_S(\vec{r}, \vec{r}')\vec{J}_S(\vec{r}') - L_W(\vec{r}, \vec{r}')\vec{J}_W(\vec{r}'). \quad (4)$$

To calculate the radiation field from the transmitter within a wide frequency band, the following techniques were implemented to reduce the computing time:

- To get the matrix $[Z]$ in (2), one needs to calculate the interaction between two RWG basic functions. Each RWG basis function is defined on a pair of connected triangles/segments, so that one needs to calculate the interactions between two triangles/segments and another two triangles/segments. This is called the *unknown-based* interactions. Instead, by using the half-RWG basis functions in Equation (3), one only needs to calculate the interaction between one single triangle/segment and another single triangle/segment. This is called *element-based* interactions. Hence, the computing time of filling $[Z]$ is greatly reduced.
- To get the volume electromagnetic field distribution inside the closed environment, one needs repeatedly calculate the integrals of (4). On the other hand, Equations (1) and (2) only need to be solved for one time to get the working parameters of the transmitting and receiving antennas. Therefore, we separate the algorithm into the processing part which solves Equations (1), (2) and the post-processing part which solves Equation (4). By this way, our implementation is more efficient than the available commercial MoM-based software where Equations (1), (2), and (4) are solved as a whole system.

2.2. Long Distance Coupling between a Pair of Transmitter and Receiver

Using a ray tracing technique suitable for UTD-based deterministic propagation model, the long distance coupling between a pair of transmitter Tx and receiver Rx is calculated based on the equivalent sources/receivers obtained from the MoM solution. In the first place, the database structures including geometric and electromagnetic model is developed. The whole structure is discretised by using planar facet. Each facet is modeled as a multilayered structure with different electromagnetic properties [16]. The propagation of the electromagnetic field is modeled as rays. The main coupling between a pair of transmitter and receiver is thus obtained as the contribution from different rays: direct ray, reflected ray, transmitted ray, diffracted ray, and their combinations. In a closed environment, the direct rays and multi-reflected rays contribute more to the couplings than the diffracted rays. This is different from the open space, where the diffracted rays are the major contribution in the shadow region. Because the strength of the diffracted ray is weak, second and higher-order diffractions are neglected.

Whenever a ray hits a discontinuity (e.g., edges, facets), reflected, transmitted or diffracted rays are generated. The generated rays continue to propagate and will produce new reflected and transmitted rays if discontinuity is encountered. This process is repeated until a maximum number of interactions have reached or until the variation of field strengths at the receiver has become smaller than a specific threshold value.

The field contribution at the observation point O due to the direct ray is given by

$$\vec{E}(O) = \vec{A}_0 \frac{e^{-jkr}}{r}, \tag{5}$$

where $\vec{A}_0$ is the antenna characteristics, and r is the distance to the Tx.

The transmitted and reflected field after transmitting through and reflecting from a facet, respectively, are given by

$$\vec{E}(O) = \vec{A}_0 \bar{T} \frac{e^{-jkr}}{r}, \quad \vec{E}(O) = \vec{E}(P) \bar{R} \frac{e^{-jks}}{s}, \tag{6}$$

where $\vec{E}(P)$ is the incident field at the reflection point P; s is the distance between O and P; $\bar{T}$ and $\bar{R}$ are the 2×2 transmission and reflection matrices, respectively, in the local ray-fixed coordinate system

$$\bar{T} = \begin{bmatrix} T_{\perp} & 0 \\ 0 & T_{//} \end{bmatrix}, \quad \bar{R} = \begin{bmatrix} R_{\perp} & 0 \\ 0 & R_{//} \end{bmatrix}, \tag{7}$$

where $\bar{T}_{\perp,//}$ and $\bar{R}_{\perp,//}$ are the transmission and reflection coefficients for the soft and hard field components, respectively [17, 18].

The UTD is applied to calculate the diffracted field by an edge

$$\vec{E}(O) = \vec{E}(Q)\bar{D}\sqrt{\frac{s'}{s(s'+s)}}e^{-jks}, \tag{8}$$

where $\vec{E}(Q)$ is the incident field at the diffraction point Q; s' and s are the distances from the Tx and the observation point O to the diffraction point Q, respectively. By using the edge-fixed coordinate system, the diffraction matrix $\bar{D}$ is given by

$$\bar{D} = \begin{bmatrix} -D_{\perp} & 0 \\ 0 & -D_{//} \end{bmatrix}, \tag{9}$$

where $\bar{D}_{\perp,//}$ are the diffraction coefficients for the soft and hard field components, respectively. These coefficients can be calculated by using the wedge diffraction coefficients modified for finite conductivity [19–21].

The received electric field is calculated as a vector sum of the individual contributions associated with the rays

$$\vec{E}_R = \sum_{i=1}^{N} \vec{E}_i, \tag{10}$$

where N is the number of paths and $\vec{E}_i$ is the complex valued electric field due to the ith ray path. It is straightforward to predict the radio coverage map by coherently combining the power of each ray path to determine the total received power.

There are two efficient propagation models for ray tracing technique: the Shooting and Bouncing Rays and the Imaging Method. In our approach, the Imaging Method has been applied because it is more efficient for analysis of geometries formed by planar facets. The Tx and Rx are modeled as points at discrete locations within the closed environment. All possible ray paths that leave Tx and arrive at Rx are calculated by determining the location of an image in each reflecting facet as shown in Figure 2. Given the maximum number of reflections, the images can be arranged in a tree graph called the images tree which is constructed in the backward procedure [16]. The same process is applied for the combination of reflected-diffracted rays, with the diffraction point taken as a suitable source to obtain an image. The diffraction point is calculated by using the edges of the model. After the ray path is found, the UTD is used to evaluate the field values for each ray.

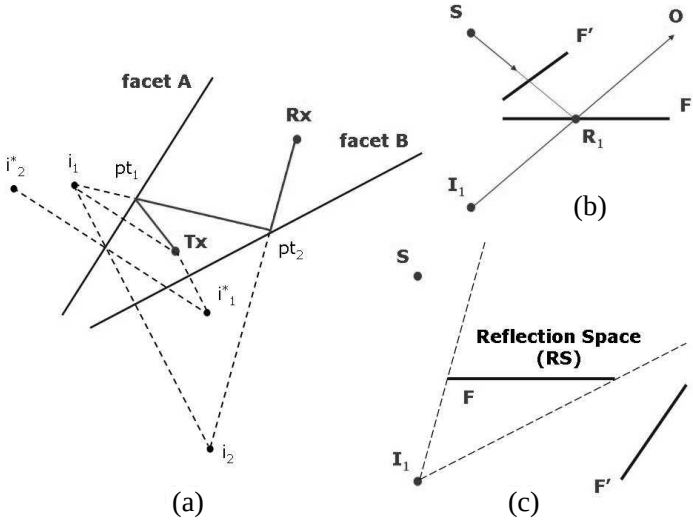

Figure 2. Imaging Method with multiples reflections.

It should be noted that the procedure to determine if any object of the scene blocks a given ray path from a source point to an observation point, is the most time consuming for ray tracing. This shadowing judgment requires a number of ray-facet intersection tests for each ray path. If the closed environment is modeled by a large number of facets, it is necessary to develop the acceleration algorithm [22].

The Binary Space Partitioning (BSP) acceleration algorithm, which is largely adopted in computer graphics, is proposed to speed up the ray tracing [23]. The basic idea of this algorithm is to build a binary tree, which represents the visibility relationship between the facets of the environment. The shadowing test is carried out based on the relative positions of the source point and the observation point with respect to the tree knot. The process is repeated until the whole BSP tree is investigated. It should be noted that the BSP algorithm is independent with the locations of Tx and Rx. This feature is thus very useful in ray tracing for the various image sources. An alternative acceleration algorithm for ray tracing, so-called Angular Z-Buffer (AZB) has also been developed. This algorithm is based on the light buffer technique that derives from the computer graphics, often used for rendering more complex scenes [24, 25].

3. VALIDATION

In order to validate the proposed simulation technique, several numerical examples are given. The first example consists of a simple model representing a corridor and a vertically polarized disc-cone antenna placed inside the corridor as shown in Figure 3. The electric field distribution within the corridor is investigated along a trajectory. At high frequency of 3 GHz, the proposed structure is electrically large to be solved using traditional full-wave method (i.e., MoM, FDTD . . .). The commercial software FEKO which is based on the Multilevel Fast Multipole Method (MLFMM) is employed for the simulation.

Figure 3 shows the simulated results, and a good agreement can be observed between the proposed hybrid simulation technique (denoted as Hybrid) and the MLFMM. It should be noted that, our technique requires much less CPU time and memory used than the MLFMM as shown in Table 1. Some discrepancies appear at the observation points nearby the walls, which are produced by near-field coupling of the antenna.

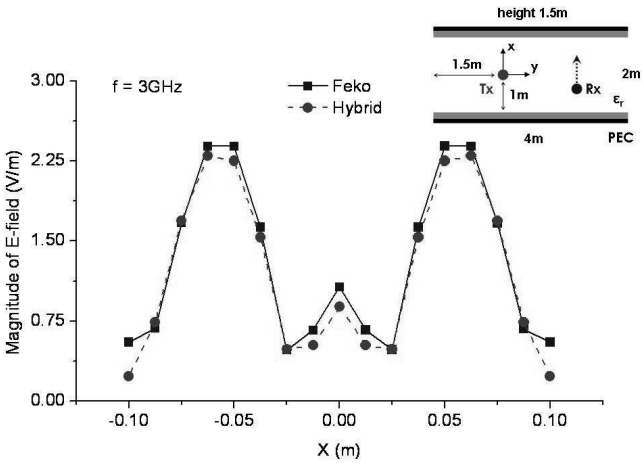

Figure 3. Comparison between our hybrid model and FEKO — Electric field strength distributed along X direction at the receiving points $(x_r, y_r, z_r) = (X, 1.5, 0.0)$. Transmitting antenna is located at the origin of the coordinate system. The dimensions of the corridor are of $2 \times 4 \times 1.5$. The structure is geometrically symmetric with respect to the XY and YZ planes. All dimensions are in meter. The corridor is made by PEC-backed coating wall with $\varepsilon_r = 4$, $\sigma = 0.01\,\mathrm{S/m}$, and coating thickness $d = 0.005\,\mathrm{m}$. Multiple reflections due to walls are taken into account.

Table 1. Comparison of memory requirements and CPU time – Corridor model.

Technique	Memory requirements [MB]	CPU time [sec]
MLFMM (Feko)	4000	1800
Hybrid	10	150

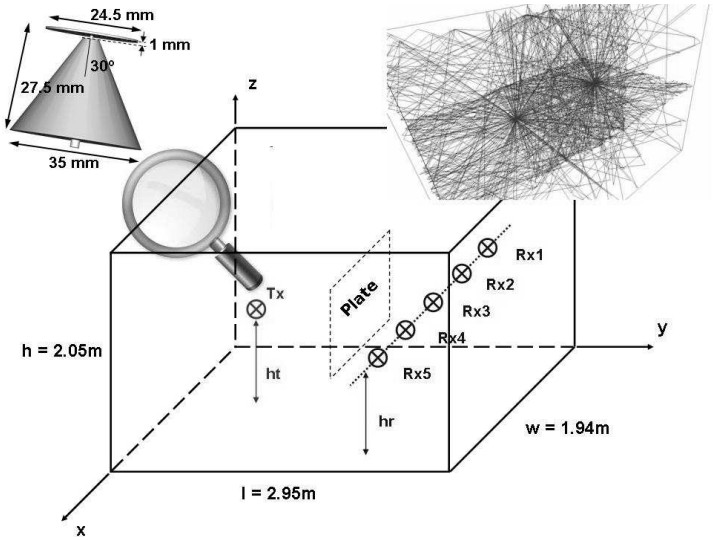

Figure 4. An enclosed room made by metal wall ($\sigma = 11000\,\mathrm{S/m}$) with dimensions of 1.94 width, 2.95 length, and 2.05 height. A metal plate with dimensions of 0.94×1 placed at $(x_{pmin} - x_{pmax}, y_p, z_{pmin} - z_{pmax}) = (0.5 - 1.44, 1.75, 0.5 - 1.5)$ used as furniture placed inside this room to block the Line-Of-Sight (LOS) between transmitting antenna and the receiving points. All dimensions are in meter.

Figure 4 shows an enclosed room equipped with furniture that is proposed as the second example. A vertically polarized disc-cone working at frequency of 3 GHz which is again used as transmitting antenna fixed inside the room. We then investigate the electric field distribution along a line. Furthermore, the effect of metallic furniture on the field strength is also investigated by adding a plate between the transmitting antenna and the observation points. Given its dimension, this plate creates a Non Line-Of-Sight (NLOS) region for all observation points. In this case, the diffraction from the edge of the plate is considered.

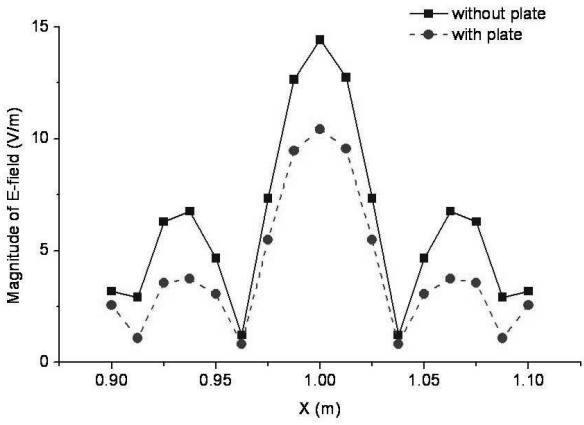

Figure 5. Comparison between the models with and without plate — Magnitude of the electric field along X direction at $(x_r, y_r, z_r) = (X, 2.25, 1.0)$. Transmitting antenna is located at coordinates $(x_t, y_t, z_t) = (0.97, 1, 1)$. All dimensions are in meter.

In an enclosed room, multiple reflections from walls are the dominant propagation mechanisms. Hence, it is necessary to conduct the convergence prediction to set the appropriate number of reflections for such a closed scenario. In the simulations, the direct, reflected, transmitted, diffracted rays were all included as shown partially in Figure 4 (upper right).

The simulation of such electrically large structure is a big challenge for FEKO, even using the MLFMM. On the other hand, the strong multi-reflections in the enclosed space make it very hard for the iterative solver of the MLFMM to obtain the convergence. Figure 5 shows the simulated results without or with plate by using the hybrid model. We observe that there are several strong paths besides the Line-Of-Sight (LOS) component which do not fade significantly. Back-tracing of the strongest multipaths revealed that they result from reflections at the walls. As expected, the field values at the calculated points are attenuated in the presence of added plate. However, the attenuation is not so significant. The reason is that the reflected rays can bypass the plate and reach the observation points. Their contribution is mostly higher than the diffracted rays arriving at the same point. The effect of furniture thus plays an important role in determining the electric field distribution inside an enclosed room.

We then set up a measurement campaign to validate the proposed hybrid simulation technique. The measurements were conducted inside

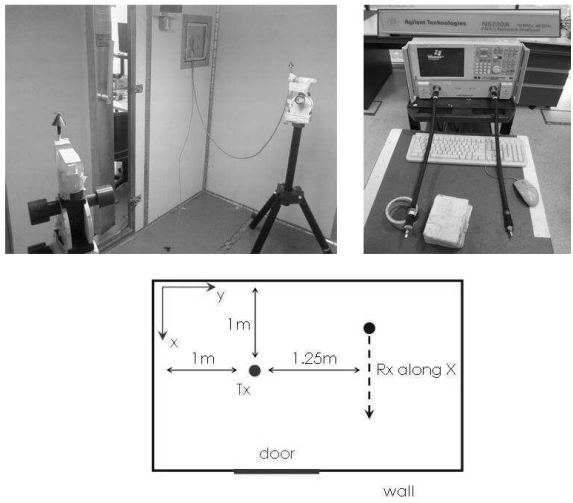

Figure 6. Measurements conducted for the signal propagation between two disc-cones inside a shielding room by using a Vector Network Analyzer (HP 8753E), which generates the transmitted power ($P_t = -10\,\text{dBm}$) and captures the signal at the receiver over the entire measurement frequency (2.8 GHz to 3.2 GHz). The 2D cut-plane shows the locations of the Tx and Rx according to the origin of the coordinate system. Tx and Rx are above the floor at the same height of 1 m.

a shielding room as shown in Figure 6. The dimensions of this room are of 1.94 m width $\times$ 2.95 m length $\times$ 2.05 m height, the same as the simulated model in Figure 4. The wall is made of galvanize steel. The assumed wall equivalent conductivity is of $\sigma_{eq} = 11000\,\text{S/m}$. The conductivity is indeed equivalent in the sense that it accounts for all loss mechanisms (wall joints, small apertures, door contacts and so on). Two vertically polarized disc-cone antennas are used as transmitting and receiving antennas. The transmitter Tx was fixed within the room. The receiver Rx is moved to capture the signals along a trajectory. During the measurement, only the tripod stands supporting the antennas are placed inside the room. The rest of the measuring equipment is linked via phase-stable co-axial cables to the outside. The measurements were carried out several times a day and over days. We found that the reading on the spot is rather stable except at some locations. The inconsistence comes in because it is difficult to locate to exact position every time we have shifted the receiver, and several uncertainties such as cable layout, location, human body movement, temperature, measurement setting and calibration.

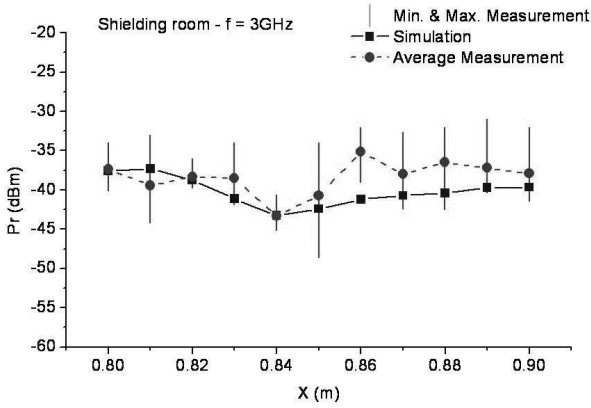

Figure 7. Comparison between the simulated results and the measurements (averaged value/range of the minimum and maximum values) — Received power in dBm recorded along X direction.

The comparison between the simulations and measurements is plotted as shown in Figure 7. A good correlation can be seen as the simulated received signals mostly lie in the range of the measured values. Hence, the prediction obtained is acceptable for the EMC application purpose. The difference between the measurement and simulation is due to that the material properties of real walls are different from their theoretical values; and the shape of the room is approximately simulated in our hybrid model.

4. CONCLUSION

In this paper, a hybrid simulation technique has been developed for analysis of the electromagnetic field interactions between multi-transmitters and receivers located within a closed environment. In our hybrid scheme, the MoM is used to accurately model the transceivers and their nearby regions. The results obtained from the MoM solution are then taken as the equivalent sources/receivers and substituted into the long-distance coupling calculation between a pair of transmitter and receiver, by using an approach that combines the UTD with the Imaging Method. The BSP acceleration algorithm has been developed for ray tracing to reduce the intensive computation of the complex scenarios.

The simulated results of electric field distribution within a corridor and inside an enclosed room with or without metallic objects have

shown that our proposed technique is accurate and efficient. The electric field strength inside a closed environment is much greater than the free-space field strength because of a large number of reflections of signals from the walls and other interior structures. The multiple reflections are thus the main coupling in a closed environment. Taken into account the uncertainties, the comparisons for the received power in dBm between the simulations and the measurements conducted within the shielding room are in good correlation.

The field coverage within an enclosed space is very sensitive to small changes in physical structure, loading (material, personal, and equipment), temperature, etc. over a period of time. Therefore, it is also necessary to derive the statistical distribution models. Further work should include the movement such as human body into the model to describe the dynamic scenario. Moving effect can be considered as multi-static model and affect only small and local region. The developed simulation technique appears to be very promising for EMC analysis.

REFERENCES

1. Nguyen, T. X., S. V. Koppen, J. J. Ely, G. N. Szatkowski, J. J. Mielnik, and M. T. P. Salud, "Small aircraft RF interference path loss," *Proc. IEEE International Symposium on Electromagnetic Compatibility*, 2007.
2. Debono, C. J. and R. Farrugia, "Optimization of the UMTS network radio coverage on-board an aircraft," *Proc. of the 2008 IEEE Aerospace Conference*, Mar. 2008.
3. Zhai, H. Q., S. Y. Jung, and M. Y. Lu, "Wireless communication in boxes with metallic enclosure based on time-reversal ultra-wideband technique: A full-wave numerical study," *Progress In Electromagnetics Research*, Vol. 101, 63–74, 2010.
4. Constantine, A. Balanis, *Antenna Theory: Analysis and Design*, 2nd Edition, John Wiley & Sons, 1997.
5. Chew, W. C., *Fast and Efficient Algorithms in Computational Electromagnetics*, Artech House, Boston, MA, 2001.
6. Sahalos, J. N. and G. A. Thiele, "On the application of the GTD-MM technique and its limitations," *IEEE Transactions on Antennas and Propagation*, Vol. 29, 780786, Sep. 1981.
7. Bouche, D. P., F. A. Molinet, and R. Mittra, "Asymptotic and hybrid techniques for electromagnetic scattering," *Proc. IEEE*, Vol. 81, 1658–1684, Dec. 1993.
8. Chou, H.-T. and H.-T. Hsu, "Hybridization of simulation codes

based on numerical high and low frequency techniques for the efficient antenna design in the presence of electrically large and complex structures," *Progress In Electromagnetics Research*, Vol. 78, 173–187, 2008

9. Medgyesi-Mitschang, L. N. and D.-S. Wang, "Hybrid methods in computational electromagnetics: A review," *Computer Physics Communications*, Vol. 68, 76–94, 1991.
10. Hsu, H.-T., F.-Y. Kuo, and H.-T. Chou, "Convergence study of current sampling profiles for antenna design in the presence of electrically large and complex platforms using FIT-UTD hybridization approach," *Progress In Electromagnetics Research*, Vol. 99, 195–209, 2009.
11. Wei, X. C. and E. P. Li, "Efficient EMC simulation of enclosures with apertures residing in an electrically large platform using the MM-UTD method," *IEEE Trans. Electromagn. Compat.*, Vol. 47, No. 4, 717–722, Nov. 2005.
12. Quijano, A. J. L. and G. Vecchi, "Field and source equivalence in source reconstruction on 3D surfaces," *Progress In Electromagnetics Research*, Vol. 103, 67–100, 2010.
13. Rao, S. M., D. R. Wilton, and A. W. Glisson, "Electromagnetic scattering by surfaces of arbitrary shape," *IEEE Transactions on Antennas and Propagation*, Vol. 30, No. 3, 409–418, May 1982.
14. Araujo, M. G., J. M. Bertolo, F. Obelleiro, J. L. Rodriguez, J. M. Taboada, and L. Landesa, "Geometry based preconditioner for radiation problems involving wire and surface basis functions," *Progress In Electromagnetics Research*, Vol. 93, 29–40, 2009.
15. Medgyesi-Mitschang, L. N. and J. M. Putnam, "Integral equation formulations for imperfectly conducting scatterers," *IEEE Transactions on Antennas and Propagation*, Vol. 33, No. 2, Feb. 1985.
16. Cátedra, M. F. and J. Pérez, *Cell Planning for Wireless Communications*, Artech House, Reading, MA, 1999.
17. Chew, W. C., *Waves and Fields in Inhomogeneous Media*, IEEE Press, New York, 1995.
18. Lin, Z. W., X. J. Zhang, and G. Y. Fang, "Theoretical model of electromagnetic scattering from 3D multi-layer dielectric media with slightly rough surfaces," *Progress In Electromagnetics Research*, Vol. 96, 37–62, 2009.
19. Kouyoumjian, R. G. and P. H. Pathak, "A uniform geometrical theory of diffraction for an edge in a perfectly conducting surface," *Proc. IEEE*, Vol. 62, 1448–1461, Nov. 1974.

20. Luebbers, R. J., "Finite conductivity uniform GTD versus knife edge diffraction in prediction of propagation path loss," *IEEE Transactions on Antennas and Propagation*, Vol. 32, No. 1, 70–76, Jan. 1984.
21. Burnside, W. D. and K. W. Burgener, "High frequency scattering by a thin lossless dielectric slab," *IEEE Transactions on Antennas and Propagation*, Vol. 31, 104–110, Jan. 1983.
22. Kim, H. and H. Lee, "Accelerated three dimensional ray tracing techniques using ray frustums for wireless propagation models," *Progress In Electromagnetics Research*, Vol. 96, 21–36, 2009.
23. Foley, J. D., A. V. Dam, S. K. Feiner, and J. F. Hughes, *Computer Graphics: Principles and Practice*, 2nd Edition, Addison-Wesley, New York, 1996.
24. Zha, F.-T., S.-X. Gong, Y.-X. Xu, Y. Guan, and W. Jiang, "Fast shadowing technique for electrically large targets using Z-buffer," *Journal of Electromagnetic Waves and Applications*, Vol. 23, No. 2–3, 341–349, 2009.
25. De Adana, F. S., O. G. Blanco, I. G. Diego, J. P. Arriaga, and M. F. Cátedra, "Propagation model based on ray tracing for the design of personal communication systems in indoor environments," *IEEE Transactions on Antennas and Propagation*, Vol. 49, No. 6, Nov. 2000.